Polymer Bulletin 33, 505–512 (1994)

Polymer Bulletin

The influence of asymmetric lateral branching in the flexible spacer on the properties of a main-chain thermotropic liquid crystal polyester

J. del Pino, C. Marco*, G. Ellis, M. A. Gómez, and J. G. Fatou

Instituto de Ciencia y Tecnología de Polímeros, C.S.I.C., c/Juan de la Cierva 3, E-28006-Madrid, Spain

Summary

The synthesis and characterisation of the thermotropic polyester poly[oxy-(1,4-dimethyltetramethylene)oxycarbonyl-3-chloro-1,4-phenyleneoxyterephthaloyloxy-2-chloro-1,4-phenylenecarbonyl] is described, and its thermal behaviour analysed. The effect of asymmetrical substitution in the tetramethylene spacer is analysed and the polymer compared with its non-substituted homologue. Substitution of methylene units at the 1,4 positions in the spacer results in a considerable lowering of the both the transition temperatures and the associated molar enthalpies, and inhibits the formation of three-dimensional order.

Introduction

In recent years, main-chain liquid crystal polymers have been the object of an important amount of attention, directed fundamentally towards establishing relationships between structure and properties (1-6). In particular, the thermotropic polyesters are one group of liquid crystals in which much interest and research has been focussed. Consequently, structural variables such as the length and structure of both the mesogenic unit and the spacer, the odd or even number of methylene units in the flexible spacer, the amount and type of substitution in the mesogen, molecular weight and thermal history, control in a fundamental way the properties of these materials. Amongst the thermotropic polyesters, one of the most important series is that in which the mesogenic unit is made up of 4,4'-terephthaloyldioxydibenzoic acid, whose synthesis and characterisation has been reported in the literature for polymers with linear spacers of between 3 and 12 methylene units (7-12), as well as the kinetics of the phase transitions (13). However, even with flexible spacers, some of these polyesters present very high transition temperatures, and considerable interest exists in reducing these temperatures in order to favour the industrial applications of these materials. In this respect, substituents of different size and polarity have been incorporated onto the aromatic units of the mesogen (7,14-19). Very recently, the effect of symmetrical substitution of methyl groups in linear trimethylene spacers has been studied (20), and a series of studies incorporating lateral substituents in the flexible spacer of liquid crystal polymers which present chiral properties have been reported (21-24). The presence of this type of substituent in the spacer induces the spatial separation of the mesogenic units and, as well as reducing the transition temperatures, can lead to the loss of three-dimensional order.

The main objective of this study, as part of a general project on the study of structure-property relationships in poly(alkylene 4,4'-terephthaloyldioxydibenzoate)s, is to describe for the first time the synthesis and characterisation of poly[oxy-(1,4-dimethyltetramethylene)oxycarbonyl-3-chloro-1,4-phenyleneoxyterephthaloyloxy-2-chloro-1,4-phenylenecarbonyl], P1, and its thermal transitions, analysing the effect of asymmetric substitution in the tetramethylene spacer, and to compare the results with those obtained from the corresponding polyester with a linear tetramethylene spacer.

Experimental

Synthesis and characterisation

Polyester, P1, was synthesised in three stages in accordance with the method described by Bilibin *et*

* Corresponding author

al. (25-27). It was characterised using elemental analysis, ^{1}H-NMR, ^{13}C-NMR, and vibrational spectroscopy. The results of the elemental analysis were the following:

Found,	%C 60.34; %H 3.98; %Cl 12.72
Calculated,	%C 60.53; %H 3.99; %Cl 13.08

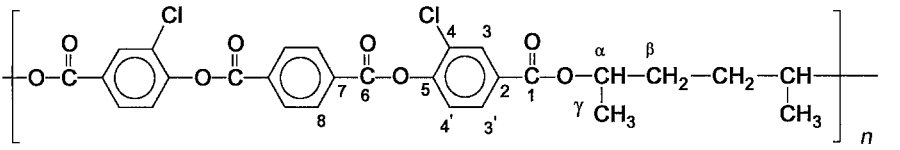

Polyester P1

The ^{1}H-NMR and ^{13}C-NMR spectra were recorded on a Varian XL-300, in $CDCl_3$ and CF_3COOH solutions, respectively, at room temperature. The ^{1}H-NMR spectrum shows the following chemical shifts (see formula for notation):

δ (ppm from TMS): δ_8 = 8,61 (4H); δ_3 = 8,38 (2H); $\delta_{3'}$ = 8,25-8,22 (2H, d); $\delta_{4'}$ = 7,62-7,60 (2H, d); δ_α = 5,44 (2H, m); δ_β = 2,05 (4H, m); δ_γ = 1,61-1,59 (6H, d).

The ^{13}C-NMR spectrum shows the following chemical shifts (see formula for notation):

δ (ppm from TMS): δ_6 = 166,87; δ_1 = 165,40; δ_5 = 150,19; δ_7 = 132,18; $\delta_{3'}$ = 131,29; δ_8 = 130,07; $\delta_{3,4}$ = 128,82; δ_2 = 127,12; $\delta_{4'}$ = 122,92; δ_α = 74,28; δ_β = 30,45; δ_γ = 17,35.

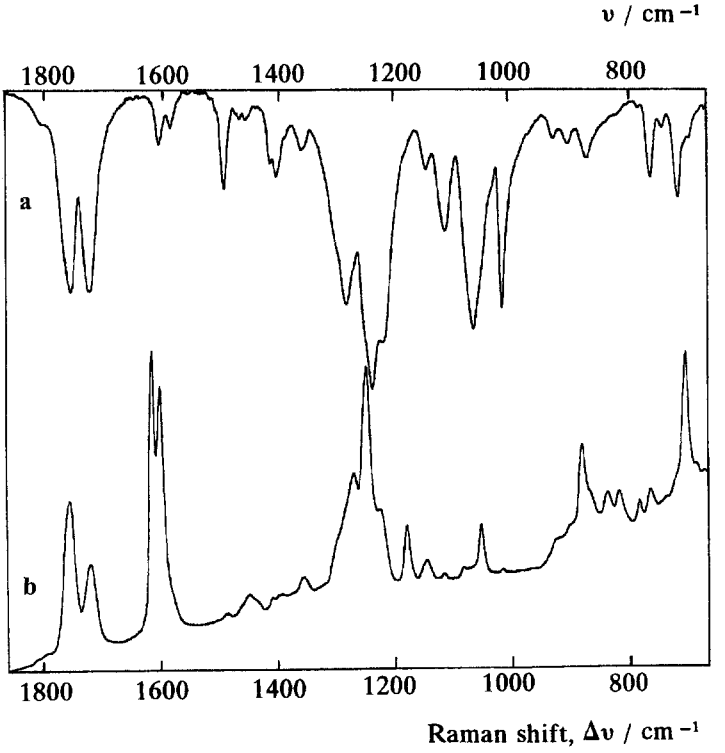

Figure 1. Vibrational spectrum of polyester P1: (a) FT-IR, (b) FT-Raman.

The vibrational spectrum was recorded on a Perkin Elmer System 2000 combined FT-IR / FT-Raman instrument. In the Raman mode, an InGaAs detector was used at room temperature, and laser excitation was provided by a Spectron Model SL-301 Nd^{3+}:YAG laser at $\nu_0 = 9493$ cm^{-1}, with a laser power of 100 mW incident on approximately 10 mg of the original polymer sample. A total of 200 scans were accumulated at a resolution of 4 cm^{-1}. The FT-Raman spectra were corrected for the optical characteristics of the instrument (28). In the IR mode, a deuterated triglycine sulphide (D-TGS) detector was used. The sample was prepared as a KBr disk, and 50 scans were accumulated at a resolution of 4cm^{-1}. The vibrational spectra were processed on a PC using IRDM-2 software.

The vibrational spectrum recorded from the original sample is presented, between 1900 - 600 cm^{-1}, in Figure 1. Characteristic band frequencies are observed in both the FT-IR and FT-Raman spectra. The symmetric and anti-symmetric CH_3 stretching modes appear at 2970 and 2870 cm^{-1} can be clearly distinguished from the comparable CH_2 stretching vibrations at 2935 and 2853 cm^{-1}, and the aromatic C-H stretching vibrations between 3100 - 3020 cm^{-1}. The CH_2 and CH_3 deformation modes are observed weakly between 1500 - 1320 cm^{-1} (bending, wagging) and between 900 - 800 cm^{-1} (rocking), the vibrational spectrum being dominated by the stronger vibrations of the aromatic nuclei, with modes observed at, for example, 1490, 1420, 1400, 837, 817, 760, 640 and 630 cm^{-1}. In the carbonyl stretching region two distinct band groups are observed, corresponding to the terephthaloyl (1780 - 1740 cm^{-1}) and oxybenzoyl (1740 - 1700 cm^{-1}) C=O stretching vibrations. The strongest bands in the FT-Raman spectrum correspond to the symmetric quadrant stretching modes of the aromatic rings, at 1613 cm^{-1} (terephthalate) and 1559 cm^{-1} (oxybenzoate), the latter being displaced to lower frequency compared with non-substituted polymers (10), due to the chlorine atom at the *ortho* position in the oxybenzoate rings. In the infrared spectrum, these modes are only active for the non-centrosymmetric oxybenzoate rings. The region between 1320 - 1200 cm^{-1} is complex in both spectroscopic techniques, with bands arising from a combination of vibrations including those due to the aromatic nuclei, ring-C(=O), C-O-C and (O=)C-O stretches. The medium intensity ring-Cl stretching vibration is observed in the FT-Raman spectrum at 1051 cm^{-1}, and appears strongly as a shoulder at around 1049 cm^{-1} in the infrared spectrum (29).

The inherent viscosity of the polymer was measured in an Ubbelohde viscometer at a concentration of 0.5 $g \cdot dL^{-1}$ in *p*-chlorophenol at 45°C.

Physical properties

Thermogravimetric analysis was realised using a Mettler TG-50 thermobalance, with a nitrogen purge, at a heating rate of $10°C \cdot min^{-1}$.

The thermal transitions were determined using a Mettler TA-4000 differential scanning calorimeter, with a DC-30 oven, coupled to a PC with TA-72 thermal analysis software. The heating and cooling rate was $10°C \cdot min^{-1}$, taking the peak maximum as the transition temperature, and the mid-point in the case of the glass transition temperature.

Wide angle x-ray diffractograms were recorded with a Phillips Geiger counter x-ray diffractometer using an Anton Paar 300 temperature cell, in the range between $2\theta = 2$ to 35° using Ni-filtered CuK_α radiation at $2° \cdot min^{-1}$.

Thermooptical analysis was performed using a Reichert Zetopan polarised light microscope, with a Mettler FP-80HT hot stage and a Nikkon FX35A camara.

Results and discussion

The polyester, P1, was synthesised for the first time, using the method described by Bilibin *et al.* for other members of this series (25-27), and that used previously by our research group to obtain homologous thermotropic polyesters with symmetrical and asymmetrical substitution in the flexible spacer (20,30). It allows one to obtain highly pure polymers with perfectly defined chemical structure, as confirmed by the results of the elemental analysis, vibrational spectroscopy and ^{1}H-NMR and ^{13}C-NMR spectroscopy.

The inherent viscosity of P1 in *p*-chlorophenol at 45°C was found to be 0.29 $dL \cdot g^{-1}$, which is comparable to that of 0.39 $dL \cdot g^{-1}$ reported for the corresponding polyester with a linear spacer,

poly(oxytetramethylene-oxycarbonyl-3-chloro-1,4-phenylene-oxyterepthaloyloxy-2-chloro-1,4-phenylenecarbonyl), P2, under the same conditions (19).

Figure 2 presents a series of DSC curves recorded for P1 with different thermal treatments. In the case of the original sample (i.e. the white powder obtained from the reaction mixture by precipitation and washing with ethanol, and dried under vacuum), two endothermic transitions can be observed, in Figure 2a, at 133°C and 176°C, with enthalpies of 7.0 and 4.6 $J \cdot g^{-1}$ respectively. It is important to indicate that the wide-angle x-ray diffractogram of this original sample at room temperature presents two main reflections at 2θ = 14.2 and 24.3°, which correspond with three-dimensional order in the material, Figure 3a, and indicate a crystallinity value of around 15%. Consequently, the endothermic transition at 133°C corresponds with the crystal - liquid crystal transition, and that at 176°C with the liquid crystal - isotropic transition, as confirmed by the observation of the clearing point in the thermooptic analysis, shown in Figure 4.

In the x-ray diffractograms recorded as a function of temperature, a reduction in the intensity of the two reflections previously mentioned is observed at 120°C, indicating the start of the loss of crystalline order in the transformation to the mesophase, Figure 3b. These reflections disappear completely at 150°C, leaving an amorphous halo centred at 2θ = 20°, which corresponds with a nematic mesophase, Figure 3c. At the higher temperature of 200°C the diffractogram is that of the isotropic fluid, Figure 3d.

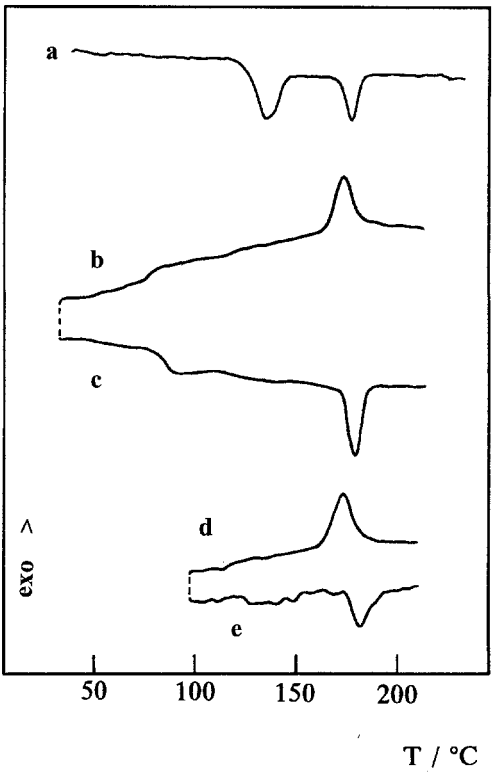

Figure 2. DSC curves of P1: (a) Original sample heated up to 250°C, (b) Cooling down from 210°C to room temperature, (c) Sample "b" heated up to 210°C, (d) Cooling from 210°C to 95°C, (e) Sample maintained at 95°C for 14h., (f) Heating curve after the anealing process, at $2°C \cdot min^{-1}$.

Table 1: Thermal transitions and thermodynamical parameters of P1 and P2

SAMPLE	T_g (°C)	T_i (°C)	ΔH_i ($J \cdot g^{-1}$)	T_i (°C)	ΔH_i ($J \cdot g^{-1}$)
a	-	133	7.0	176	4.6
b	77	-	-	171	7.0
c	77	-	-	183	4.9
P2[a]	-	274	4.0	319	8.0

(a) Reference 19.

When the original sample is heated to the isotropic state and then cooled at 10°C·min^{-1}, only a single exothermic transition is observed at 171°C, with an enthalpy of 7.0 J·g^{-1}, which corresponds with the transition from the isotropic state to the mesophase, followed at lower temperatures by a variation in the baseline at 77°C, with a change in the specific heat of 0.15 J·g^{-1}·K^{-1}, which is due to the glass transition, with no apparent evidence in the thermogram of the formation of any three-dimensional order. The same behaviour is observed when the original sample is heated to and cooled from the mesophase, with only the glass transition being detected. In the subsequent heating cycle, Figure 2c, the glass transition is once more observed, followed by a very broad endothermic transition of very low enthalpy, which extends almost up to the mesophase - isotropic transition. Table 1 presents a summary of the transition temperatures and enthalpies observed in Figure 2.

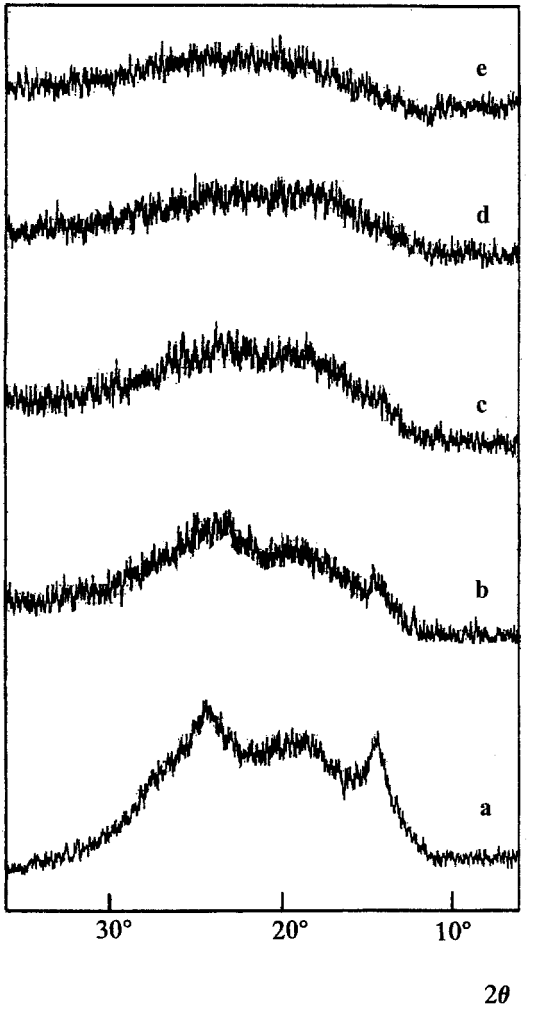

Figure 3. X-ray diffractograms of P1: (a) Room temperature, (b) 110°C, (c) 120°C, (d) 150°C, (e) 200°C.

The x-ray diffractogram of P1 recorded at room temperature, after cooling from either the mesophase or from the isotropic state, does not show the reflections characteristic of the three-dimensional order previously observed, implying that once the sample has melted, to either an anisotropic or isotropic state, the order present in the original material is not be recovered on cooling. In order to investigate the possibility of the generation of crystalline order, a sample of P1 was cooled from the isotropic melt at 210°C, at a rate of 10°C·min^{-1}, to a temperature of 100°C, above the glass transition temperature and below the value of T_1 observed in the first heating cycle, where it was maintained for 14 hours, Figures 2d and 2e. The subsequent heating curve, recorded at 2°C·min^{-1}, Figure 2f, shows what appears to be the generation of three-dimensional order, represented by a very broad endotherm between 123 and 153°C, with an enthalpy of approximately 2.6 J·g^{-1}. This is followed by the isotropisation, T_i at 174°C, with an enthalpy of 8.4 J·g^{-1}.

In order to confirm these results, thermooptical analysis of films prepared by cooling from both the mesophase and the isotropic state was undertaken. At room temperature the polarised light micrographs of these films show a striped texture of alternately light and dark stripes in a parallel distribution, Figure 5a. These are anologous to the structures denominated Williams domains, found

in Kevlar fibres and oriented aromatic polyamide films (31-36), and in a variety of thermotropic polyesters, without the application of magnetic fields (37-40). When the films are heated at a velocity of 10°C·min^{-1}, Figure 4a, a variation in the luminous intensity is observed between 120 and 140°C, which continues almost up to the clearing point. This evolution in the luminous intensity almost coincides with the disappearance of the Williams stripes, and the subsequent development of a marbled nematic texture with areas of different molecular orientation, Figure 5b. Close to T_i a texture consisting of droplets with Schlieren type residues can be distinguished, up to isotropisation, Figure 5d.

When the polyester P1 is cooled from the isotropic melt, Figure 4b, an initial gain in the luminous intensity is observed, which corresponds to the formation of the nematic mesophase, which progressively diminishes in intensity until room temperature is reached. The phenomenon of the variation of the nematic mesophase is repeated in the subsequent heating cycle, up to the mesophase, Figure 4c, and in the subsequent thermooptic cycles, Figures 4d and 4e.

The fact that the nematic mesophase presents an important variation in its texture, in a temperature interval which practically coincides with the broad and extended endothermic process in the corresponding DSC thermogram, Figure 2c, seems to indicate that during the cooling process in P1, a certain amount of three-dimensional order is introduced into the sample.

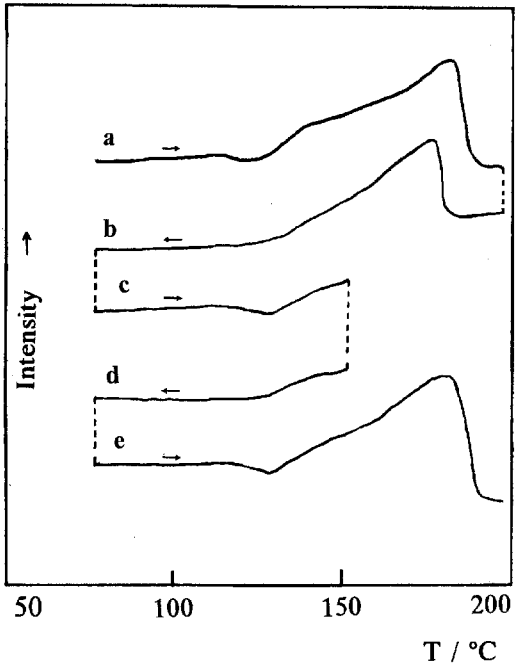

Figure 4. Thermooptical analysis of P1: (a) Sample heated up to, (b) Cooling cycle after "a", (c) Heating cycle up to 150°C, (d) Cooling cycle from 150°C, (e) Sample heated up to 195°C after "d".

The polyester P1 shows the crystal - liquid crystal transition, T_l, at a temperature 141°C lower than that for polyester P2 (19), with the same mesogenic unit and the linear tetramethylene spacer, Table 1. A reduction of the same order, 143°C, is observed for T_i, and the mesophase is stable over more or less the same temperature interval for both P1 and P2. The differences in the phase diagrams of these polyesters cannot be attributed exclusively to differences in molecular weight, given that the inherent viscosities are reasonably similar. Thus, it seems that the amount of substitution in the flexible spacer plays an important role in the molecular packing. Although there is little data in the literature on the influence of lateral substituents in the flexible spacer on the thermal transitions, previous indications that the presence of methyl and ethyl substituents in a linear spacer provoke important reductions in the transition temperatures have been reported (20,30,41). For example, the symmetical substitution of two methyl and two ethyl groups in the trimethylene spacer of poly(1,5-dioxopentamethylenecarbonyl-*p*-terphenyl-4,4′-diylcarbonyl) reduces the isotropisation temperature by 57 and 205°C, respectively. In another case, the symmetrical substitution of a dimethyl group in poly(oxytrimethylene-oxycarbonyl-1,4-phenylene-oxyterephthaloyloxy-1,4-phenylenecarbonyl) provokes a reduction in the crystal - mesophase I, mesophase I - mesophase II and mesophase II - isotropic transitions, from 240, 265 and 272°C to 100, 160 and 210°C respectively (20). In the case of the polyester P1, with asymmetric substitution of two

methyl groups in positions 1 and 4 of the linear tetramethylene spacer, the strong steric limitations in the molecular packing are not only manifested in a lowering of the transition temperatures, but also in the molar enthalpy values associated with the T_1 transition, $21.2 \cdot 10^3$ and $3.9 \cdot 10^3$ $J \cdot mol^{-1}$, and the T_i transition, 38.6 and 9.5 $J \cdot mol^{-1}K^{-1}$, for P2 (linear) and P1 (branched) respectively, taking into account that in both cases the mesophases are nematic (19). The same behaviour has been observed in homologous thermotropic polyesters without chlorine substitution in the mesogen (30,42).

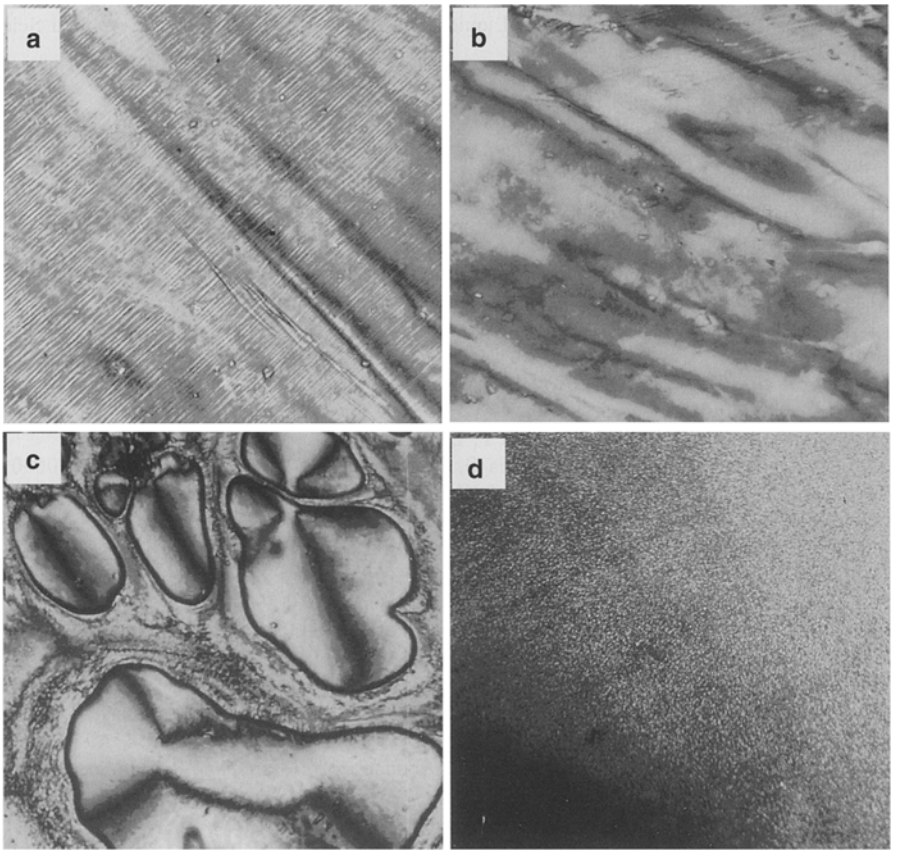

Figure 5. Microphotographs of polyester P1: (a)Williams domains at room temperature, (b) marbled texture, c) droplets, and d) isotropic state

These packing differences are also reflected in the ability to develop three-dimensional order, which appears in the case of the polyesters with linear spacers, which also present polymorphism depending on the thermal history of the material (19,42), whilst its formation is impeded in the case of the polyesters with asymmetrically branched spacers, where only a certain amount of three-dimensional order is generated in P2, and after a long annealing process (30). This impediment appears to be even greater in the case of P1, where the cooperative effect of both substitution in the mesogen and the spacer presents a greater restriction to the packing of the molecular chains.

Acknowledgements
Financial support was provided by the CICYT (Mat-91-0505) and the Comunidad Autónoma de Madrid (CO72/91). J.del P. wishes to thank the Spanish Ministerio de Educación y Ciencia for a postgraduate research grant.

References

1. Lenz R W J (1985) Polym Sci Polym Symp 72:1
2. Blumstein A Ed. " Polymeric Liquid Crystal", Plenum Press, New York (1985)
3. Economy J (1984) J Macromol Sci Chem 121: 1705
4. Chapoy L, Ed. "Recent Advances in Liquid Crystalline Polymers", Elsevier Applied Science Publisher, London (1985)
5. Cherdron H (1990) Makromol Chem Makromol Symp 33: 85
6. Percec V, Nava H (1987) J Polym Sci Polym Chem Ed 25: 405
7. Lenz R W (1985) Polym J 17: 105
8. Skorokhodov S S, Bilibin A Yu (1989) Makromol Chem Makromol Symp 26: 9
9. Marco C, Lorente J, Gómez M A, Fatou J G (1992) Polymer 33: 3108
10. Ellis G, Lorente J, Marco C, Gómez MA, Fatou J, Hendra P (1991) Spectrochim Acta 47A: 1353
11. Hudson S D, Lovinger A J, Gómez M A, Marco C, Fatou J G Macromolecules (to be published)
12. Ober C K, Delvin A, Bluhm T L (1990) J Polym Sci Polym Phys Ed 28: 1047
13. Lorente J, Marco C, Gómez M A, Fatou J G (1992) Eur Polym J 28: 911
14. Delvin A, Ober C K (1988) Polymer B 20: 45
15. Jin J I, Choi H S, Choi E J, Yoon Ch J (1990) J Polym Sci Polym Phys Ed 28: 531
16. Chen G, Lenz R W (1984) J Polym Sci Polym Chem Ed 22: 3189
17. Galli G, Chiellini E, Ober C K, Lenz R W (1982) 183: 2693
18. Nieri P, Ramireddy C, Wu C N, Munk P, Lenz R W (1992) 25: 1796
19. del Pino J, Gómez M A, Marco C, Ellis G, Fatou J G (1994) Makromol Chem 195: 0000
20. Lorente J, Marco Rocha C, Gómez M A, Fatou J G (1992) Polymer Comm 33:202
21. Chiellini E, Galli G, Carrozino S, Gallot B (1990) Macromolecules 23: 2106
22. Gallot B, Galli G, Chiellini E (1987) Makromol Chem Rap Comm 8: 417
23. Chiellini E, Galli G, Malanga C, Spassky N (1983) Polymer B 9: 336
24. Chiellini E, Neri P, Galli G (1984) Mol Cryst Liq Cryst 113: 213
25. Bilibin A Yu, Ten'kovtsev A V, Piraner O N, Skorokhodov S S (1984) Polym Sci USSR 26: 2882
26. Bilibin A Yu, Ten'kovtsev A V, Skorokhodov S S (1985) Makromol Chem Rap Comm 6: 209
27. Skorokhodov S S, Bilibin A Yu (1989) Makromol Chem Makromol Symp 26: 9
28. Petty C J, Warnes G M, Hendra P J, Judkins M (1991) Spectrochim. Acta 47A: 1179
29. Colthup N B, Daly L H, Wiberley S.E. Ed. "Introduction to Infrared and Raman Spectroscopy", Academic Press, New York (1975)
30. del Pino J, Marco Rocha C, Gómez M A, Fatou J G (1992) Makromol Chem 193: 2251
31. Dobb M G, Johnson D J, Saville D P (1977) J Polym Sci Polym Phys Ed 15: 2201
32. Chen S, Long C (1979) Polymer Comm 4: 240
33. Hu S, Xu M (1980) Polym Comm 1: 35
34. Simmens S C, Hearle J W S (1980) J Polym Sci Polym Phys Ed 18: 871
35. Li L S, Allard L F, Beglow W S (1983) J Macromol Sci Phys B22: 269
36. Panar M, Avakian P, Blume R C, Gardner K H, Gieke T D, Yang H H (1983) J Polym Sci Polym Phys Ed 21: 1955
37. Hu S, Xu M, Li J, Quian B, Wang X, Lenz R W (1985) J Polym Sci Polym Phys Ed 23: 2387
38. Lenz R W, Furukawa A, Bhownik P, Garay R D, Majnusz (1991) Polymer 32: 1703
39. Majnusz J, Lenz R W (1989) Eur Polym J 25: 847
40. Hu S, Xu M, Quian J Li, Wang X, Lenz R W, Stein R S (1988) 29: 792
41. Meurisse P, Noël C, Monnerie L, Fayolle B (1981) Br Polym J 13: 55
42. del Pino J, Gómez M A, Marco C, Ellis G, Fatou J G (1992) Macromolecules 25: 4642

Received: 23 June 1994/Accepted: 17 August 1994